JOURNAL OF CATALYSIS 134, 536–541 (1992)

An Approach to the Surface Barrier Concept in Diffusion in Zeolites by Computer Simulation

F. VIGNÉ-MAEDER, S. EL AMRANI, AND P. GÉLIN

Institut de Recherches sur la Catalyse, 2 Avenue Albert Einstein, 69626 Villeurbanne Cedex, France

Received December 17, 1990; revised September 24, 1991

The technique of molecular dynamics has been used to determine the trajectories of Ar and Xe atoms passing through the outer surface of aluminum-free MFI- and MOR-type crystals. In the case of Xe, the passage of the atom through the outer silicalite surface was observed to be significantly retarded, compared to Ar behaviour. In addition to the mass effect, this result was ascribed to a purely geometrical effect, the size of Xe and silicalite pores being comparable. Although this result qualitatively featured the behaviour of Xe in ZSM-5 measured by NMR, the model would certainly not explain the significant retardation in exchange rates observed on a macroscopic scale. A better simulation of the adsorption process, adsorbate–adsorbate interactions and energy exchange between adsorbate and surface crystal atoms taken into account, is required.

INTRODUCTION

The existence of a transport resistance at the outer surface of zeolite crystals, the so-called "surface barrier," has been postulated to explain discrepancies between uptake diffusion coefficients and NMR or neutron scattering self-diffusion coefficients (*1*). Recent ^{129}Xe NMR self-diffusion measurements demonstrated that the passage of Xe through the external surface of NaCaA and ZSM-5 zeolites was significantly retarded, strongly affecting the intracrystalline mean-square displacement (*2*). On the contrary, the molecular exchange of methane in the same zeolites was mainly controlled by intracrystalline diffusion. These results have been qualitatively related to the size difference between the adsorbed molecule and the free diameter of the zeolite pore. However, the origin of surface barrier effects, when observed, is still under debate. The partial blockage of pore apertures due to the presence of extraneous phases or structural defects (*3*) and a purely physical effect, related to an energy barrier originating in the pore aperture convexity (*4*), have been put forward.

Molecular dynamics has been proved to be a powerful tool to model the dynamic behaviour of molecules *already adsorbed* in the inner pores of zeolite crystals (*5*). Self-diffusion coefficients deduced from calculated trajectories were found to be in good agreement with those derived from pulsed field gradient NMR measurements or neutron scattering experiments (*6*). Although of the utmost relevance, no theoretical work has so far been devoted to model the trajectories of molecules sitting outside the zeolite crystal and passing through the outer surface of the crystal.

We present in this work a molecular dynamics simulation of the adsorption of rare gas atoms on zeolite crystals in order to obtain a first insight into the way adatoms penetrate the pores of zeolite crystals. The experiment consisted of defining rare gas atoms with randomly distributed velocities in the vicinity of a rigid zeolite crystal surface (siliceous MFI and MOR zeolites) and to calculate their respective trajectories. Some atoms were reflected by the outer surface: they were disregarded. Some were adsorbed on the outer surface, moved on it, and ultimately penetrated the pore of the zeolite crystal. It must be pointed out that our model suffers three strong limitations:

0021-9517/92 $3.00

(i) the adsorbate–adsorbate interactions have been neglected, a situation which corresponds to very low coverage conditions; (ii) there is no energy exchange between crystal surface atoms and adatoms; and (iii) the model surface describes an idealized surface. Consequently, it could only result in qualitative conclusions. Our results clearly show that, in addition to evident mass or surface porosity effects, size effects might be responsible for a significant retardation to Xe entering zeolite narrow pores, while not observed in the case of Ar. A better simulation of the adsorption process is, however, required to conclude on the existence of a surface barrier controlling the intracrystalline transport of Xe in MFI- and MOR-type zeolites.

METHOD

Modelling the Particle–Surface Interaction

Al-free mordenite (*7*) and MFI (*8*) zeolites have been chosen for their different pore size and network. The model surface was obtained by a clear cut of the zeolite crystal considering only the resulting surface oxygen atoms (*9*). Obviously, the outer surface of zeolite crystals built in this way represents an oversimplification of the real outer surface, covered by terminal hydroxyls and not rigorously "flat." However, it must be pointed out that considering terminal hydroxyls instead of surface oxygen atoms, while complicating the calculations, should not change significantly the interaction model because rare gas atoms do not give rise to strong hydrogen bonding. In the case of the MFI structure, the model surface, taken parallel to the [100] plane, results in grooves corresponding to sections of straight channels along the Y direction. In this model, molecules penetrate the crystal along the sinusoidal channels. The MOR model surface, parallel to the [001] plane, exhibits disconnected hollows resulting from sections of side pockets sitting perpendicularly to the channels. Ar and Xe have been chosen as the diffusing atoms to compare our results with the recent NMR studies of CH_4 and Xe diffusivities in ZSM-5 (*2*), argon and methane being shown to diffuse similarly. The adatom–zeolite interaction potential was modelled by Lennard–Jones potentials between rare gas atoms and oxygen atoms of the zeolite framework (*11*). All the oxygen atoms included in a sphere of 14-Å radius and centered at the moving particle have been considered for the interaction potential calculations.

Potential maps derived from Ar–silicalite and Ar–mordenite interactions are shown respectively in Figs. 1 and 2. Figures 1A and 2B feature the outer surface of the crystals, while Figs. 1B and 2B represent the potential distribution across the crystals (in the mirror plane along (x, y) and (y, z) directions for silicalite and mordenite, respectively). In the latter case, it must be pointed out that the areas of negative potentials do not describe the void space of the zeolite pores but the space accessible to the center of mass of the rare gas atom, which defines regions of very high potentials (appearing as obliquely hatched areas) inaccessible to Ar atoms. In figures featuring the outer surface of the crystals, pore openings have been indicated with arrows. Similar figures have been derived with Xe, differing essentially in the calculated potential values, reported as numbers in parentheses in Figs. 1 and 2.

Molecular Dynamics Simulations

Molecular dynamics simulations have been carried out in the microcanonical ensemble (constant $N\,V\,E$), which is considering N particles within a volume V of zeolite, the total energy E being constant. In our calculations, 100 independent rare gas atoms have been considered, initially localized in a plane parallel to the outer crystal surface and regularly distributed on an area equal to the unit cell side facing them. These crystal surface areas contain two pore openings for both zeolites, which therefore suppresses the influence of the surface porosity (0.0075 pore/Å^2 for silicalite and 0.0054 pore/Å^2 for mordenite). The initial veloci-

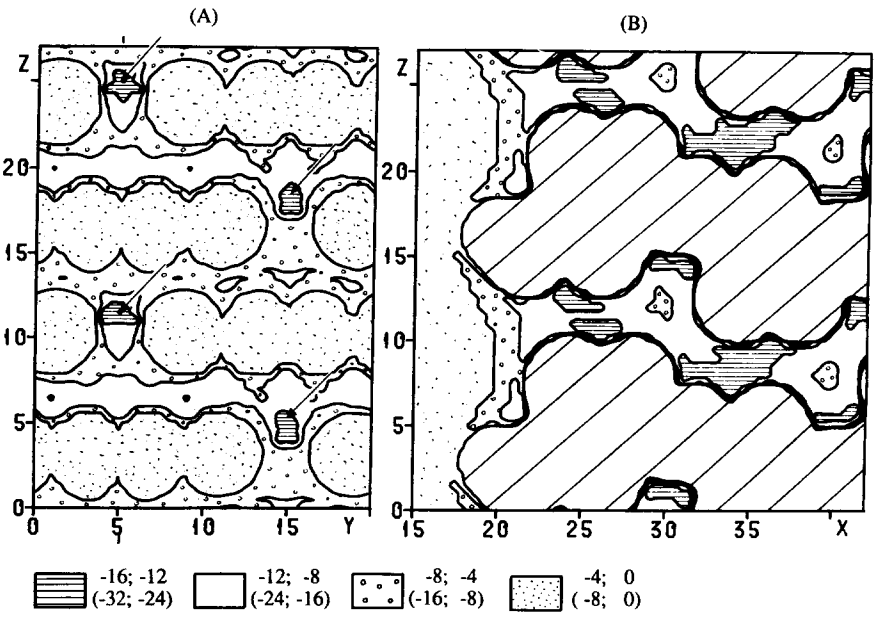

FIG. 1. Potential maps for argon and silicalite. (A) Map of the minimal potential value that can be reached by the atom approaching the external surface; (B) potential map in the mirror plane. Values in parentheses correspond to the potential maps of xenon. Energies in kJ mol^{-1}.

ties were assumed to have a Maxwell distribution corresponding to an initial mean temperature of 300 K in the gas phase. Trajectories were calculated step by step by integrating the motion equations using the Verlet algorithm. Given the positions at time

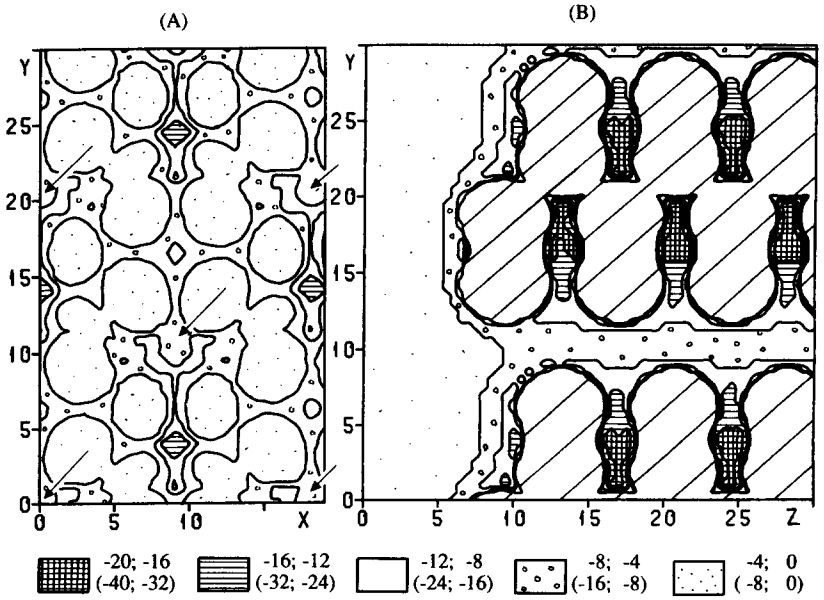

FIG. 2. Potential maps for argon and mordenite. For explanations, see Fig.1 legend.

t and $t - \delta t$, the position at time $t + \delta t$ was derived from

$$\mathbf{r}(t + \delta t) = 2\mathbf{r}(t) - \mathbf{r}(t - \delta t) + \mathbf{a}(t)\,\delta t^2.$$

The acceleration $\mathbf{a}(t)$ was related to the potential V according to

$$\mathbf{a}(t) = -(1/m)\ \mathbf{grad}\ V(\mathbf{r}(t)).$$

The trajectories of all the particles were calculated in the same run. As no interaction between rare gas atoms has been introduced in the potential V, the considered 100 atoms moved independently of each other. Time steps of 5×10^{-4} ps for Ar and 10^{-3} ps for Xe have been chosen in order to limit the total energy fluctuations to 0.03%.

A particle entering the pore opening deeper than 3 Å relative to the surface plane across the center of surface oxygen atoms was considered as "penetrating the crystal." Particles moving away from the surface plane by more than 5 Å for Ar (8 Å for Xe) were considered as no longer adsorbed and were disregarded.

Our model involved a rigid crystal, so that no energy exchange between diffusing atoms and the solid could occur. The total energy of each particle being kept constant, approaching the particle to the crystal surface where the potential energy is deeper resulted in an increase in its temperature. As a consequence, the particle had in all cases a sufficiently high kinetic energy to overcome any energy barrier and was never trapped in low potential holes of the outer surface.

RESULTS AND DISCUSSION

In Fig. 3, we report a typical trajectory of a Xe atom contacted with a mordenite model surface and its corresponding potential energy variation as a function of time. It turns out that the Xe atom had to overcome many energy barriers related to surface corrugation before entering the pore (denoted as point E in the figure). Moreover, entering the pore was not associated with a higher energy barrier, as discussed in a previous paper (*9*), which implies that the pore opening curvature would not explain the existence of a surface barrier. Table 1 clearly indicated that for the particle to move on the outer surface or inside the crystal porosity, energy barriers are close, even though surface barriers are higher than intracrystalline diffusion barriers, especially for the system Xe–silicalite.

Considering 100 diffusing particles, we

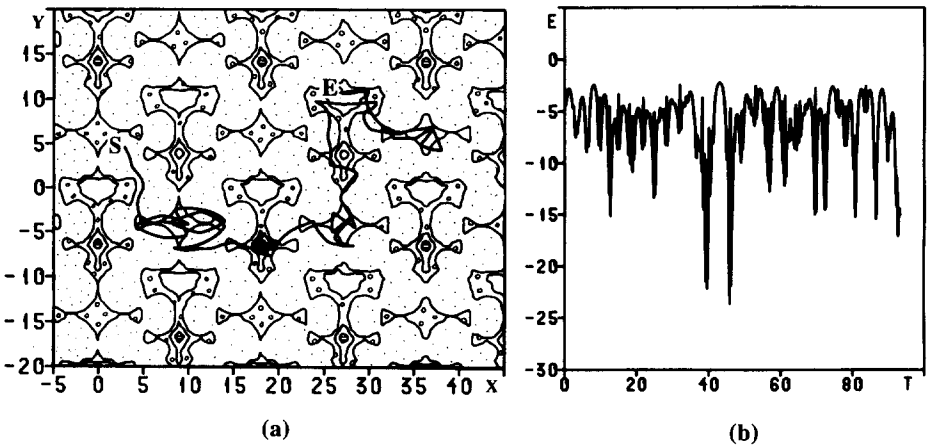

FIG. 3. Xenon on the mordenite model surface. (a) A typical trajectory superimposed with the potential distribution on the surface; (b) variation of the xenon potential energy along the trajectory (a).

TABLE 1

Energy Barriers in kJ mol^{-1} for the Diffusion of an Atom (a) on the Outer Surface or (b) Inside the Zeolite Crystal Channels

	MFI		MOR	
	(a)	(b)	(a)	(b)
Ar	10	4	10	8
Xe	22	8	22	16

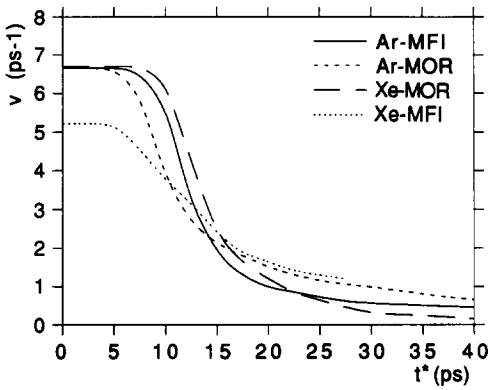

FIG. 4. Variation of the rate v at which rare gas atoms enter the zeolite pores as a function of reduced time t^*.

compare in Table 2 the number of particles of Ar and Xe finally entering the crystal porosity of MFI and MOR structures. Whatever the zeolite structure, fewer particles were reflected in the case of Xe than for Ar, in agreement with the stronger interaction of Xe with the zeolite surface. In addition, in the case of Xe, one may note a significantly larger number of particles entering the mordenite structure compared to silicalite. This might be ascribed to a larger size of mordenite pores (6.8 Å for mordenite and 5.5 Å for silicalite) in comparison to the particle diameter (4.4 Å for Xe). The effect was less sensitive in the case of Ar due to its smaller size (3.8 Å).

The rate at which the rare gas atoms entered the zeolite pores has been calculated as a function of time and has been represented in Fig. 4 for Ar and Xe in silicalite and mordenite structures. In order to take into account the mass effects between Ar and Xe, we introduced a "reduced time" t^* defined as

$$t^* = t \quad \text{for Ar}$$
$$t^* = t(m_{Ar}/m_{Xe})^{1/2} \quad \text{for Xe},$$

where m_{Ar} and m_{Xe} represent respectively the atomic masses of Ar and Xe. Therefore, the rate v at which atoms entered the pores might be defined as

$$v = (dn/dt^*)/n_\infty,$$

where n_∞ and n denote respectively the total number of atoms that have finally entered the zeolite crystal and the number of atoms that penetrated the crystal at time t^*. Two distinct parts can be distinguished in the curves reported in Fig. 4. At initial times, atoms enter the zeolite pores at a constant and high rate. Then the rate decreases drastically, corresponding to a significantly longer stay of atoms on the outer surface of the crystal. The striking feature is that all the curves are superimposed at small times, except that corresponding to the Xe–silicalite system. Several factors might affect the rate at which the atoms enter the zeolite pores, including: (i) the mass of diffusing atoms, (ii) the porosity of the surface, (iii)

TABLE 2

Number of Reflected or Entered Rare Gas Atoms

	Number of atoms		t_0(ps)	$\langle t \rangle$(ps)
	Reflected	Entered		
Ar–MFI	60	40	158	4.6
Ar–MOR	55	45	114	4.3
Xe–MFI	45	55	213	9.3
Xe–MOR	30	70	154	8.4

Note. t_{max}, Maximum time necessary for the entry into the crystal. t_0, Time separating two collisions between a particle and the outer surface of the crystal, calculated with the kinetic theory of gases. $\langle t \rangle$, Mean lifetime on the outer surface before entering the pore.

the magnitude of the potential barriers on the outer surface of the crystal, (iv) the potential distribution on the outer surface, and (v) the pore size to diffuser size ratio. The first two effects have been carefully eliminated in our way of performing calculations. Points (iii) and (iv), involving structural differences between mordenite and silicalite, should be disregarded on the basis of Ar experiments, which did not exhibit differences upon zeolite structural changes. Therefore, one should conclude that there is a size effect: Xe and silicalite pore diameters are close enough to induce a significant inhibition of Xe to enter the pore of silicalite-like structures. This effect would be of minor importance in the case of Ar due to its smaller size. Similar conclusions were reached in the NMR study of Xe and methane diffusing in ZSM-5 (*2*), where Xe was observed to exhibit significant retardation to enter the ZSM-5 pores, not evidenced for a smaller molecule (methane) or larger zeolite porosity.

From our simulations, we derived the mean residence times of diffusing atoms on the outer surface of the zeolite crystals $\langle t \rangle$, reported in Table 2 for all experiments. These values have been compared to the time separating two collisions of a particle with the outer surface, derived from the kinetic theory of gases, at a pressure of 1 atm (denoted as t_0). $\langle t \rangle$ was in all cases markedly lower than t_0, so that neglecting the interaction between particles appears to be a reasonable approximation. These values may be compared with the mean residence times of Xe or Ar atoms diffusing in the inner pores of spherical silicalite particles, derived from NMR measurements. Assuming spherical crystallites of 10 μm radius and a self-diffusion coefficient of 10^{-8} to 10^{-9} m^2 s^{-1} (*10*), the mean residence time of the particle inside the crystallite porosity may be evaluated (*12*) to be about 10^9 ps, compared to a residence time at the crystal surface calculated from our simulations of less than 10 ps. Therefore, we conclude that size effects alone are not able to explain external resistance at the surface of the zeolite crystal controlling the transport of molecules into zeolite pores. Other factors should be taken into account, in particular adsorbate–adsorbate interactions and energy exchange between adsorbate and surface, to better describe the adsorption process.

REFERENCES

1. Kocirik, M., Struve, P., Fiedler, K., and Bülow, M., *J. Chem. Soc. Faraday Trans. 1* **84,** 3001 (1988).
2. Kärger, J., Pfeifer, H., Stallmach, F., and Spindler, H., *Zeolites* **10,** 288 (1990).
3. Kärger, J., Bülow, M., Millward, G. R., and Thomas, J. M., *Zeolites* **6,** 146 (1986).
4. Derouane, E. G., André, J. M., and Lucas, A. A., *J. Catal.* **110,** 58 (1988).
5. Demontis, P., Fois, E. S., Suffritti, G. B., and Quartieri, S., *J. Phys. Chem.* **30,** 4329 (1990); Pickett, S. D., Nowak, A. K., Thomas, J. M., Peterson, B. K., Swift, J. F. P., Cheetham, A. K., den Ouden, C. J. J., Smit, B., and Post, M. F. M. *J. Phys. Chem.* **94,** 1233 (1990).
6. Jobic, H., Bée, M., Caro, J., Bülow, M., and Kärger, J., *J. Chem. Soc., Faraday Trans. 1* **85,** 4201 (1989).
7. Meier, W. M., *Z. Kristallogr.* **115,** 439 (1961).
8. Olson, D. H., Kokotailo, G. T., and Lawton, S. L., *J. Phys. Chem.* **85,** 2238 (1981).
9. Vigné-Maeder, F., *J. Catal.* **117,** 566 (1989).
10. El Amrani, S., and Vigné-Maeder, F., to be published.
11. Kiselev, A. V., Lopatkin, A. A., and Shulga, A. A., *Zeolites* **5,** 261 (1985).
12. Kärger, J., and Pfeifer, H., *Zeolites* **1,** 90 (1987).